# The Decrease in mid-Stratospheric Tropical Ozone Since 1991

Gerald E. Nedoluha[1], David E. Siskind[1], Alyn Lambert[2], and Chris Boone[3]

[1]Naval Research Laboratory, Washington, D. C., USA.

[2]Jet Propulsion Laboratory, California Institute of Technology, Pasadena, California, USA

[3]Department of Chemistry, University of Waterloo, Waterloo, Ontario, Canada.

**Abstract**

While global stratospheric $O_3$ has begun to recover, there are localized regions where $O_3$ has decreased since 1991. Specifically, we use measurements from the Halogen Occultation Experiment (HALOE) for the period 1991-2005 and the NASA/Aura Microwave Limb Sounder (MLS) for the period 2004-2013 to demonstrate a significant decrease in $O_3$ near ~10 hPa in the tropics. $O_3$ in this region is very sensitive to variations in $NO_y$, and the observed decrease can be understood as a spatially localized, yet long term increase in $NO_y$. In turn, using data from MLS and from the Atmospheric Chemistry Experiment (ACE), we show that the $NO_y$ variations are caused by decreases in $N_2O$ which are likely linked to long term variations in dynamics. To illustrate how variations in dynamics can affect $N_2O$ and $O_3$, we show that by decreasing the upwelling in the tropics, more of the $N_2O$ can photodissociate with a concomitant increase in $NO_y$ production (via $N_2O+O(^1D) \rightarrow 2NO$) at 10 hPa. Ultimately, this can cause an $O_3$ decrease of the observed magnitude.

## 1. Introduction

The slowdown in the $O_3$ decline and the beginnings of recovery of the ozone layer have been documented [*Newchurch et al.,* 2003; *Yang et al.,* 2006]. Monitoring of the ozone layer continues to be critical in order to understand ozone recovery as the CFC burden in the stratosphere decreases. A number of observational studies have quantified the global distribution of changes to the $O_3$ layer and revealed distinct patterns and variability which show that $O_3$ trends are not spatially uniform. One consistent result is that over decadal time scales, equatorial $O_3$ in a vertical layer near 30 km (corresponding to ~10 hPa) often varies very differently from $O_3$ in the rest of the middle to upper stratosphere. *Kyrola et al.* [2013], using measurements from

the Stratospheric Aerosol and Gas Experiment (SAGE) from 1984-1997, show a general decrease in $O_3$ which is statistically significant over much of the stratosphere, but an increase in equatorial $O_3$ (albeit not statistically significant) in the 30-35 km region. Conversely, for the period 1997-2011 *Kyrola et al.* [2013] show a general increase in $O_3$ from SAGE and Global Ozone Monitoring by Occultation of Stars (GOMOS) measurements, but a statistically significant decrease near 30 km in the tropics. *Bourassa et al.* [2014] combine SAGE measurements with measurements from the Optical Spectrograph and InfraRed Imager System (OSIRIS) instrument and, again splitting the data into pre- and post-1997 periods, find very similar results. *Damadeo et al.* [2014] compute a SAGE trend from 1998-2005 and find a positive trend near 30km in the tropics and Northern Hemisphere, but a negative trend in the Southern Hemisphere at this level. Measurements from the Scanning Imaging Absorption Spectrometer for Atmospheric Chartography (SCHIAMACHY) instrument for the period 2002-2012, reported by *Gebhardt et al.* [2014], show a pattern similar to the 1997-2011 pattern reported by *Kyrola et al.* [2013], i.e. a strong statistically significant decrease in tropical $O_3$ in the 30-35 km region while most of the middle atmosphere shows a slight increase in $O_3$. Finally, *Eckert et al.* [2014] using Michelson Interferometer for Passive Atmospheric Sounding (MIPAS) data from 2002-2012, also show a general increase in $O_3$ in most regions, but find statistically significant negative trends in the tropics from ~25 hPa to 5 hPa. *Eckert et al.* [2014] note that increased upwelling has been suggested as an explanation for ozone decreases, but, in referring to these trends, they conclude that "upwelling does not provide a sufficient explanation for the negative values in the tropical mid-stratosphere."

Ozone at 10 hPa over the equator is particularly sensitive to catalytic cycles involving the odd nitrogen ($NO_y$) chemical family [*Olsen et al.,* 2001; *Brasseur and Solomon,* 1986].

*Ravishankara* [2009] showed that $N_2O$ would be the dominant ozone depleting substance emitted in the 21st century, and pointed out that nitrogen oxides contribute most to $O_3$ depletion just above where the $O_3$ mixing ratios are the largest. *Portmann et al.* [2012] calculated the effects of a surface boundary increase of 20 ppbv of $N_2O$ (an increase expected over ~20 years in the IPCC A1B scenario) on $O_3$. They showed that this increase in $N_2O$ emission would lead to a global mean decrease of ~0.5-0.7% in $O_3$ just above the peak of the ozone mixing ratio (0.1 DU $km^{-1}$ in the 30-35 km region where $O_3$ has a density of ~15-20 DU $km^{-1}$ based on their Figure 2). In mixing ratio terms this gives a rate of ~5-7 ppbv/yr. *Plummer et al.* [2010] studied $O_3$ changes in a model including GHGs and ODSs. They ran two experiments with a faster Brewer-Dobson circulation, and these two experiments showed, at 10 hPa in the tropics, a decrease in reactive nitrogen and an increase in both $O_3$ and $N_2O$ at 10 hPa relative to the experiments with a slower circulation. Thus variations in $O_3$ and $N_2O$ at 10 hPa can be either correlated or anti-correlated depending upon whether they are driven primarily by circulation or by changes in $N_2O$ entering the stratosphere.

In addition to long-term anthropogenically driven changes, events such as the eruption of Mt. Pinatubo may alter the chemistry and dynamics of the stratosphere for extended periods. *Aquila* [2013] compared a reference model with a model which simulated the effect of the volcanic aerosols on both chemistry and dynamics. They calculated an increase in $O_3$ of ~2% at 10 hPa in the tropics slightly more than a year after the eruption, with no strong latitudinal variation. *Damadeo et al.* [2014] attempt to disentangle anthropogenically driven changes from Pinatubo eruption driven changes using an aerosol based volcanic proxy.

Previous observational work has correlated $O_3$ interannual variability in the tropics near 10 hPa with changes in specific odd nitrogen compounds; however, these studies were only for

relatively short time periods compared with the $O_3$ studies referenced above. *Randel et al.* [2000] showed that the Halogen Occultation Experiment (HALOE) observed increasing $NO+NO_2$ coincident with decreasing $O_3$ from 1992-1997, but that these variations leveled-off during the last years of HALOE measurements which were then available (1998-2000). The rate of $O_3$ decrease from 1992-1996 was faster than 100 ppbv/yr just above 10 hPa in the tropics. The HALOE measurements of $NO_2$ at ~10 hPa from 1993-1997 were shown to be consistent with a decrease in upward transport [*Nedoluha et al.*, 1998] and increased photolysis of $N_2O$, the source of stratospheric $NO_y$.

The present study extends the previous observational studies with a combination of 21 years of ozone data from the UARS HALOE and the Aura Microwave Limb Sounder (MLS) measurements, plus nitrogen species data from HALOE, MLS and the Atmospheric Chemistry Experiment (ACE). Our results confirm the existence of the 10 hPa tropical ozone trend anomaly and link it to a correspondingly consistent local change in the nitrogen species which affect $O_3$. The resulting rate of change in $O_3$ and in the nitrogen species is an order-of-magnitude faster than changes predicted from model calculations based upon changes in anthropogenic emissions.

## 2. Measurements from HALOE, Aura MLS, and ACE

We make use of measurements from the HALOE, MLS, and the Fourier transform spectrometer measurements from ACE. HALOE measurements of $O_3$, NO, and $NO_2$ are available from 1991-2005. HALOE used the solar occultation technique which provided ~28-30 profiles per day in two latitude bands, one at sunrise and one at sunset. The latitude bands drifted daily so that near global latitudinal coverage was provided in both sunrise and sunset

106 modes five times over the course of a year. The trends in the HALOE $O_3$ measurements have
107 been compared against SAGE II (*Nazaryan et al.*, 2005) and differences have been found to be
108 on the order of less than 0.3% per year in a majority of latitude bands at 25, 35, 45, and 55 km.
109 MLS measurements of $O_3$ and $N_2O$ are available since 2004. MLS measurements are
110 available over a global range of latitudes on a daily basis. The stratospheric $O_3$ product has been
111 validated by *Froidevaux, et al*. [2008]. The $N_2O$ measurements have been validated by *Lambert,*
112 *et al.* [2007].
113 Since 2004 ACE has been measuring $O_3$, $N_2O$, and the nitrogen species that constitute the
114 bulk of $NO_y$ (NO, $NO_2$, $HNO_3$, and $N_2O_5$). As a solar occultation instrument it, like HALOE,
115 provides ~28-30 profiles per day in two latitude bands, one at sunrise and one at sunset. The
116 ACE $O_3$ measurements have been validated by *Dupuy et al.* [2009], and the NO and $NO_2$
117 measurements were validated by *Kerzenmacher et al.* [2008].
118
119 **2.1 The Solar Cycle and Linear Trend Calculations**
120 In cases where species are affected by the solar cycle, one of the challenges in
121 interpreting decadal scale trends in the stratosphere is separating these trends from solar cycle
122 induced variations. Model studies provide some guidance as to the expected solar cycle
123 variations in the species of interest. *Egorova et al.* [2005] used the SOCOL Chemistry Climate
124 Model (CCM) and found that at 30 km $O_3$ was higher at solar maximum when compared to solar
125 minimum, but that the difference was <3%. The $N_2O$ mixing ratio at 30 km from $30^oS$-$30^oN$ was
126 found to be no more than 2% higher at solar minimum compared to solar maximum, and no more
127 4% from $30^oN$-$60^oN$ and $30^oS$-$60^oS$. Schmidt et al. [2010] used the HAMMONIA general
128 circulation and chemistry model, and found an equatorial $O_3$ sensitivity of ~1.4+/-0.4%/100 solar

129 flux units (sfu), where the difference between the 1989 solar max and the 1986 solar min is 166
130 sfu. The study of *Remsberg and Lingenfelser* [2010] shows a 3% ozone maximum-minimum
131 response to the solar cycle at ~35 km (~7 hPa) from the SAGE II measurements, with results
132 from the HALOE measurements and from model calculations showing a smaller ozone response
133 to the solar cycle. As discussed in *Hood and Soukharev* [2006], $NO_y$ in the upper stratosphere is
134 also affected by the solar cycle. They place an upper limit of ~10% on the solar cycle variations
135 in $NO_y$ in the tropical mid-stratosphere. The model calculations in *Egorova et al.* [2005] show
136 an $NO_2$ solar cycle variation of <1%, and *Nedoluha et al.* [1998] show a similarly small variation
137 from the CHEM2D model (*Bacmeister et al.*,1998).

138 Throughout this study we will calculate trends based on a function including terms to fit
139 the annual, semi-annual, QBO, plus a constant term and a linear trend term. The QBO terms
140 were calculated using the Center for Climate Prediction 30 hPa and 50 hPa winds anomalies
141 obtained from www.cpc.ncep.noaa.gov/data/indices/. In addition to these terms we have
142 calculated trends from the HALOE measurements both with and without the inclusion of a solar
143 cycle term, where the solar cycle fit is calculated using the Mg II values obtained from the
144 Laboratory for Atmospheric and Space Physics (LASP) Interactive Solar Irradiance Datacenter
145 at lasp.colorado.edu/lisird. We will only show HALOE trend calculations where a solar cycle
146 term has been included, but we have compared trends with and without the solar cycle term and
147 found that the results are similar.

148 The MLS measurement time series used here extends from 2004-2014, and therefore
149 clearly does not extend over a full solar cycle. The linear trend calculations from MLS
150 measurements which will be shown cover the period August 2004 to May 2013. Because Solar
151 Cycle 24 is particularly weak the Mg II values in 2013 are comparable to those in 2004, so solar

effects are unlikely to cause a trend in the MLS dataset used here. In order to provide an estimate of the uncertainty in the trend which is introduced by the presence of a solar cycle we will show some MLS results both with and without the inclusion of a solar cycle term. We will show that in the region of greatest interest, near the tropics at ~10 hPa, the MLS trends appear to be nearly insensitive to the presence of a solar cycle.

### 2.2 Measurements of $O_3$, 1991-2014

In Figure 1 we show the annual median $O_3$ anomalies from $5^oS$-$5^oN$ as measured by both HALOE and Aura MLS at 10 hPa. This figure also shows that the $O_3$ decrease at 10 hPa has occurred gradually over the period shown. There have been numerous studies combining $O_3$ timeseries from multiple satellites to derive long-term trends (e.g. *Jones et al.*, 2009; *Kyrola et al.*, 2013), and there are several projects underway to provide long-term data records of stratospheric composition, so we will not attempt here to produce a combined HALOE-MLS $O_3$ timeseries for trend calculations. The MLS timeseries anomalies shown have simply been offset by a shift in mixing ratio so that the anomaly point for 2005 (which covers data taken during the period July 2004 through June 2005) agrees with the HALOE anomaly at that point. The anomalies are calculated by fitting annual and semi-annual cycles to each dataset separately and then calculating annual median differences from this fit. The annual anomaly is sampled four times per year so that each point represents an anomaly over either January-December, April-March, July-June, or October-September. Each measurement is therefore included in four data points in the figure. Having removed the annual cycle, the primary variation in $O_3$ in this region is caused by the QBO. In addition to these QBO variations there is a clear decrease in $O_3$ over the 21 years shown.

An estimate of the uncertainty in these annual medians can be obtained from the standard deviation of the individual anomalies. The average value of $\sigma/n^{1/2}$ for the annual median HALOE $O_3$ anomalies is 0.026 ppmv. The last annual anomaly has the largest uncertainty with $\sigma/n^{1/2}$=0.056ppmv. For the MLS, which has many more measurements, the largest annual median uncertainty calculated by this method is 0.0027 ppmv.

In Figure 2 we show the linear trend in the global HALOE ozone measurements from 1991-2005. Remsberg [2008] show a quite similar figure (their Figure 13) for linear trends in HALOE $O_3$, but in %/decade. They found that the trends near 10 hPa from ~25$^o$S to ~25$^o$N had a confidence interval of >90% for their partial tank order correlations (Remsberg et al., 2001). The trend is negative (i.e. $O_3$ is decreasing) near ~10 hPa with the most negative values occurring in the tropics. Most of this study will focus primarily on the causes of this $O_3$ decrease in this region. In general the results are very similar whether or not a solar cycle is included in the fit, but the local tropical minimum at ~4 hPa does not appear when such a term is not included.

HALOE measurements ceased in 2005, and Aura MLS has been providing $O_3$ measurements since 2004. In Figure 3 we show the linear trend in $O_3$ as measured by MLS. MLS shows that the negative ozone trend in the tropics near ~10 hPa continued from August 2004 to June 2013. Inclusion of the most recent MLS data (from July 2013 to Sept. 2014) does not result in a qualitative change in Figure 3, but does reduce the magnitude of the measured trends. Again, the $O_3$ linear trends shown in Figure 3 have been calculated with a solar cycle included in the fit, but the results are very similar with and without a solar cycle term. Several other datasets have also shown decreasing $O_3$ near 10 hPa in the tropics. *Kyrola et al.* [2013] has shown a decrease for 1997-2011 from SAGE and GOMOS, *Gebhardt et al.* [2014] for 2002-

198 2012 using measurements from SCIAMACHY, and *Eckert et al.* [2014] for 2002-2012 using
199 MIPAS measurements. There is some overlap between the negative HALOE $O_3$ trend (1991-
200 2005) and the positive SAGE $O_3$ trend shown by [*Kyrola et al.,* 2013] (1984-1997). Given the
201 excellent agreement between SAGE II and HALOE trends [e.g. *Nazaryan et al.,* 2005], and the
202 eruption of Mt. Pinatubo near the middle of the 1984-1997 timeseries, we expect this difference
203 between the 1984-1997 and 1991-2005 trends is caused by a real change in $O_3$ trends in the
204 tropical 10 hPa region in between 1991 and 1997.

205 While Figure 1 shows a general decrease in $O_3$ at 10 hPa over the entire HALOE
206 measurement period, and Figure 3 shows that this trend continued into the MLS measurements
207 period, such trends do not always persist over such extended periods. For example, away from
208 the tropics the 1991-2005 HALOE and 2004-2013 MLS trends near 10 hPa show clear,
209 hemispherically dependent, differences. Whereas the HALOE trends show a decrease in $O_3$ at
210 all latitudes near 10 hPa, the MLS trends show a sharp increase in $O_3$ at Southern mid-latitudes,
211 and a smaller decrease at similar pressure levels in Northern mid-latitudes.

212 Just as the HALOE and MLS trends show clear differences away from the tropics, they
213 also show clear differences in the tropics at other levels. The 1991-2005 HALOE trend shows an
214 increase in tropical $O_3$ near 30 hPa, but this is dominated by the strong increase from ~1991-
215 1999, followed by a period of stability in this region from 1999-2005. The MLS $O_3$
216 measurements suggest that this period of stability near 30 hPa continues through 2013. However
217 *Gebhardt et al.* [2014] do show statistically significant $O_3$ increases in the 2002-2012
218 SCIAMACHY measurements below 30 km with two local maxima, one near 22 km and one near
219 27 km, while *Eckert et al.* [2014] show an $O_3$ increase from 2002-2012 near 22 km (~50 hPa)
220 but a decrease near 27 km (~25 hPa) from the MIPAS measurements. In their 1984-1997 $O_3$

221 trends *Kyrola et al.* [2013] show an increase at 24 km, but a much larger decrease at 21 km.
222 Thus, while several measurements show decadal scale tropical trends near 10 hPa, such trends to
223 not appear to be common near 30 hPa, nor at other latitudes near 10 hPa.
224
225 **2.3 The Effect of Changes in Nitrogen Species on Ozone**
226 As noted above, $O_3$ in the tropical mid-stratosphere is particularly sensitive to changes in
227 $NO_y$ which result from photodissociation and oxidation of $N_2O$ [*Olsen et al.*, 2001], and long-
228 term *increases* in anthropogenic $N_2O$ emission are expected to play a significant role in causing
229 future *decreases* in $O_3$ [*Portman et al.*, 2012]. However, $N_2O$ is also a sensitive indicator of
230 upward transport and, as we show below, these variations in transport lead to a positive, not
231 negative correlation between $N_2O$ and $O_3$. Figure 4 presents the correlation between MLS $N_2O$
232 and $O_3$ from 2004-2013. These correlations are calculated by first finding a zonal monthly
233 median for each year of MLS data and then subtracting from each of these the average MLS
234 monthly median for that month. Note the strongly positive correlation precisely where the
235 observed long term trends indicate ozone decreases. Figure 5 presents monthly median MLS
236 $N_2O$ and $O_3$ data from $5^oS$-$5^oN$ at 10 hPa. The positive correlation between $N_2O$ and $O_3$ is clearly
237 present on seasonal and interannual timescales and rules out an anthropogenic increase in $N_2O$ as
238 the cause of the long term ozone decreases we observe.
239 This positive correlation between $N_2O$ and $O_3$ in the tropical middle stratosphere can be
240 readily understood in the context of the relationship between $N_2O$, $NO_y$ and $O_3$. This is
241 demonstrated in Figure 6 which presents ACE measurements of $O_3$, $N_2O$ and the species which
242 make up the bulk of $NO_y$ at 30 km (~10 hPa) from $10^oS$-$10^oN$. While ACE does not provide the
243 daily measurement coverage in the tropics obtained by MLS, it does measure all of the species

244 relevant to the nitrogen chemistry which determines $O_3$ near ~10 hPa in the tropics. Like MLS,
245 ACE shows a strong positive correlation between $N_2O$ and ozone. ACE also shows the expected
246 anticorrelation resulting from the chemistry of $O_3$ and $NO_y$. Figure 6c shows the anti-correlation
247 between $NO_y$ and $N_2O$ without which the correlation between $N_2O$ and $O_3$ would not exist. This
248 anti-correlation of $N_2O$ and $NO_y$ can be understood as a coupled chemical/dynamical effect.
249 During periods when upward transport is slower, more $N_2O$ at a given altitude is dissociated,
250 thus producing more $NO_y$ at that altitude. We thus conclude that over the period of the MLS
251 measurements the effect of changes in transport on $N_2O$ in this region on $NO_y$ and hence $O_3$
252 dominate any increase in $N_2O$ due to changing tropospheric emissions.

253 As indicated in Section 2.1, the MLS instrument has been operational for less than a full
254 solar cycle; hence for tropical trend calculations we show results both with and without the
255 inclusion of a solar cycle term. In Figure 7 we show the calculated profiles as a function of
256 pressure as derived from eight (constant term, two annual terms, two semi-annual terms, two
257 QBO terms, and a linear trend) and nine (including a solar cycle) parameter fits to the monthly
258 median MLS measurements. Figure 7 shows the profiles (the constant terms from the fits) in
259 addition to the linear trend and the net effect of 8 years of such a trend (2004-5 vs. 2012-13).
260 The $O_3$ trend results are in good agreement with those shown by *Gebhardt et al.* [2013] for
261 August 2004-April 2012, where the fastest decreasing trend in MLS $O_3$ is ~7%/decade.
262 *Gebhardt et al.* [2013] show that the MLS trends in $O_3$ are not statistically different from those
263 observed by SCIAMACHY or OSIRIS. While the inclusion of the solar cycle term fit clearly
264 does affect the linear trend at some levels, it does not alter the qualitative result that $O_3$ and $N_2O$
265 both show a statistically significant decrease over a similar range of pressures near 10 hPa. This

266 further reinforces the conclusion that this decrease in $O_3$ is caused by an increase in $NO_y$
267 (resulting from increased dissociation of $N_2O$) during this period.

268 As was shown in Figure 2, HALOE measurements showed a decrease in $O_3$ from 1992-
269 2005 at 10 hPa from $5^oS$-$5^oN$. While HALOE did not provide measurements of $N_2O$, and did not
270 provide the full complement of $NO_y$ species that is available from ACE, it did provide
271 measurements of two of the key odd-nitrogen species, NO and $NO_2$.

272 In Figure 8 we show annual median HALOE anomalies in $O_3$ alongside those of
273 $NO+NO_2$. Because $NO+NO_2$ has a strong diurnal component (unlike the set of $NO_y$
274 measurements provided by ACE), the anomalies for both species are calculated separately for
275 sunrise and sunset measurements. We have multiplied the sunset $NO+NO_2$ measurements by 0.4
276 so that they fit onto the same scale as the sunrise measurements. The average (maximum) $\sigma/n^{1/2}$
277 value for sunrise $NO+NO_2$ is 0.064 ppbv (0.082 ppbv), while for the sunset measurements
278 (before multiplication by 0.4) it is 0.122 ppbv (0.22 ppbv). For the $O_3$ sunrise measurements the
279 average (maximum) $\sigma/n^{1/2}$ value is 0.045 ppmv (0.064 ppmv), while for the sunset measurements
280 it is 0.049 ppmv (0.081 ppmv).

281 Figure 8 shows that $NO+NO_2$ generally was increasing over the course of the HALOE
282 measurements and that this increase tracked the ozone decrease, both on a year-to-year timescale
283 (dominated by the quasi-biennial oscillation, QBO) and over the full 1992-2005 time period.
284 There is a slight (~3-month) apparent phase-lag between the sunset and sunrise $NO+NO_2$
285 measurements from ~1998-2003 which is not apparent in the $O_3$ anomalies and for which we
286 have no explanation. With the exception of this feature, the general consistency between the
287 QBO driven variations in $O_3$ and $NO+NO_2$, and the trend which is apparent in both the $O_3$ and
288 $NO+NO_2$ measurements, provides added confidence that the decrease in $O_3$ and the increase in

289 $NO+NO_2$ measured by HALOE from 1992-2005 are both correct and, further, are coupled. As
290 we concluded from the MLS measurements from 2004-2013, this change suggests a slowdown in
291 upward transport in this region from 1992-2005. Note, this is consistent with the results of
292 *Nedoluha et al*. [1998] who interpreted the decreases in upper stratospheric $CH_4$ from 1992-1996
293 as linked with a simultaneous increase in $NO_2$ at 30 km. Our results here extend that early result
294 to encompass the entire 13 year UARS mission.

295 In Figure 9 we show the calculated linear trends in the HALOE $O_3$ and $NO+NO_2$
296 measurements. As in Figure 8 we separate the HALOE sunrise and sunset measurements, and
297 calculate trends for four separate measurements: sunrise and sunset $O_3$ and sunrise and sunset
298 $NO+NO_2$. Encouragingly, despite having very different vertical profiles, the shape of the sunrise
299 and sunset $NO+NO_2$ trend profiles are very similar. The $O_3$ sunrise and sunset trends also agree
300 well, and the pressure level of the minimum of the observed decrease in these $O_3$ measurements
301 corresponds closely with the maximum in the observed increase in the $NO+NO_2$ measurements.
302

303 **3. Model Calculations**

304 In order to better understand the changes in the observed species we have employed the
305 two-dimensional chemical transport model (CHEM2D) (*Bacmeister et al.,* 1998). The model
306 includes parameterized gravity wave and planetary wave drag and is ideal for understanding
307 tracer transport and the response of the global middle atmospheric circulation to external
308 forcings. Compared with those earlier studies, the present model has an improved vertical
309 resolution (1 km instead of 2 km). CHEM2D's most recent applications have included
310 simulating the solar cycle variations of polar mesospheric clouds (*Siskind et al.,* 2005) and

311 studying the response of stratospheric ozone to both the solar cycle and the tropical quasi-
312 biennial oscillation (*McCormack et al.,* 2007)

313 We will show results from two model runs, each of which has been integrated for 12
314 years to ensure stability from year-to-year. Since the goal of the model was to test whether
315 dynamical changes would affect $N_2O$, $NO_y$, and $O_3$ at the equator, we introduced a very simple
316 perturbation. The two models differ only in that, in one case, we added a small heat source of
317 0.3 K/day, centered at 18 km at the equator, similar to Experiment 7 of *Bacmeister et al* (1998).
318 In addition, we recognize that the model differences shown represent two equilibrium solutions
319 while the calculated trends show the effects of an atmosphere changing over time. Nonetheless,
320 a comparison of these two models can serve as an indication whether it is possible to reproduce
321 the observed changes in the measured species with a dynamical perturbation.

322 Figure 10 shows the change in $N_2O$, $NO_y$, and $O_3$ at the equator resulting from this
323 dynamical perturbation. The absolute values for these three species at 10 hPa are in very good
324 general agreement with those shown in Figure 6 from the ACE measurements. The $N_2O$
325 chemistry is relatively simple, and $N_2O$ at all levels is lower for the case of the slower tropical
326 ascent which offers more time for dissociation. At 10 hPa the case with the slower ascent shows
327 ~22 ppbv less $N_2O$. Unlike the measurements, however, the $N_2O$ in the model changes over a
328 deep layer, covering the entire pressure range from 50-1hPa.

329 The calculated equatorial $N_2O$ changes shown in Figure 10 correspond with calculated $O_3$
330 and $NO_y$ profile changes which are in the same sense and general magnitude as the observations.
331 Thus the calculation with lower $N_2O$ yields increased $NO_y$ due to increased oxidation. via
332 $N_2O+O(1D) \rightarrow 2NO$; the baseline model with ~22 ppbv less $N_2O$ shows an increase of ~1.3
333 ppbv in $NO_y$, so $\Delta NO_y/\Delta N_2O$ ~0.065. This is similar to the $\Delta NO_y/\Delta N_2O$ in the ACE

measurements in Figure 6c, which is ~.075. Regarding ozone, the baseline model with less heating and 1.3 ppbv greater $NO_y$ shows about ~0.26 ppmv less $O_3$ at 10 hPa. This yields a $\Delta O_3/\Delta NO_y$ of ~200 which is on the order of, but somewhat less than, the observed $\Delta O_3/\Delta NO_y$ from the ACE measurements (which is closer to ~330). We can also directly compare the calculated quantity $\Delta O_3/\Delta N_2O$ in the model and in the ACE and MLS measurements; here we also get a somewhat reduced ozone response compared with the observations. Whereas the model shows a $\Delta O_3/\Delta N_2O$ of ~12, ACE and MLS both show $\Delta O_3/\Delta N_2O$ ~25). About 25% of this difference is because the model $\Delta NO_y/\Delta N_2O$ sensitivity is slightly less than observed. Also, since our approach towards diurnal averaging requires a specific of a single night-to-day ratio (cf. *Summers et al.,* 1996) it is possible that we are underestimating the diurnally averaged response of $O_3$ to $NO_x$ chemistry, which varies strongly with the time of day. Nevertheless, the qualitative agreement between the model and the ACE and MLS measurements supports the idea that the observed $O_3$ change can be caused by a dynamical perturbation.

While the model runs do support the suggestion that the changes in $O_3$ and $N_2O$ observed near the equator at ~10 hPa can be caused by a dynamical perturbation, we do note that this particular dynamical perturbation also shows large differences in other regions where the measured trends are small and/or vary in a temporally different manner than do the tropical 10 hPa measurements. No doubt a number of dynamical changes affected $N_2O$ over the period 1991-2013, and these variations drove changes in $NO_x$ and in turn $O_3$. What we conclude here is that, because of changes in transport, the $N_2O$ which arrived in this region experienced significantly more dissociation in 2013 than in 2004, and, based on inferences from the HALOE $O_3$ and $NO_x$ measurements, that this trend was also present throughout much of the HALOE measurement period. We note that there is a burgeoning literature debating the possibility of

changes in the stratospheric circulation [cf. *Butchart*, 2014 and references therein]. The results presented here may serve as a useful constraint for these analyses of long term stratospheric variability.

## 4. Summary

Ozone measurements from HALOE and MLS show a long-term decrease in $O_3$ in the tropical mid-stratosphere near the peak of the $O_3$ mixing ratio. $O_3$ in this region is very sensitive to variations in $NO_y$, and the observed decrease in $O_3$ can be understood in terms of the effects of increasing $NO_y$. From MLS and ACE measurements we conclude that the $NO_y$ variations are the result of a decrease in $N_2O$ from 1992-2012 resulting from changes in the dynamics over this period. Using a 2D model, we show that a perturbation of the dynamics results in changes in $N_2O$, $NO_y$, and $O_3$ which are qualitatively consistent with the observed trends. In future it would be interesting to study $N_2O$, $NO_y$, and $O_3$ variations in this region in more sophisticated 3D models.

A feature of particular interest for future work is the increase in $O_3$ observed in the Southern Hemisphere mid-stratosphere by MLS. Both the overall increase in $O_3$ in this region as well as the short-timescale variations are well correlated with changes in $N_2O$, suggesting that this $O_3$ variation is also dynamically controlled.

**Acknowledgments.** This project was funded by NASA under the Upper Atmosphere Research Program, by the Naval Research Laboratory, and by the Office of Naval Research. Work at the Jet Propulsion Laboratory, California Institute of Technology, was carried out under a contract with the National Aeronautics and Space Administration. MLS and HALOE data are available

from the NASA Goddard Earth Science Data Information and Services Center (acdisc.gsfc.nasa.gov). ACE-FTS data is available at www.ace.uwaterloo.ca.

**References**


Aquila, V., et al, The Response of Ozone and Nitrogen Dioxide to the Eruption of Mt. Pinatubo at Southern and Northern Midlatitudes (2013), J. Atmos. Sci., 70, 894-900.

Bacmeister, J. T., D. E. Siskind, M. E. Summers, and S. D. Eckermann, (1998) Age of air in a zonally averaged two-dimensional model, J. Geophys. Res., 103, D10, 11263-11288.

Bourassa, A E., D. A. Degenstein, W. J. Randel, J. M. Zawodny, E. Kyrola, C. A. McLinden, C. E. Sioris, and C. Z. Roth (2014), Trends in stratospheric ozone derived from merged SAGE II and Odin-OSIRIS satellite observations, Atmos. Chem. Phys., 14, 6983–6994, 2014.

Brasseur, G. P. and S. Solomon (1986), Aeronomy of the Middle Atmosphere, D.Reidel press.

Butchart, N., The Brewer-Dobson circulation (2014), Rev. Geophys., 52, 157–184, doi:10.1002/2013RG000448.

Damadeo, R. P., J. M. Zawodny, and L. W. Thompson (2014), Reevaluation of stratospheric ozone trends from SAGE II data using a simultaneous temporal and spatial analysis, Atmos. Chem. Phys., 14, 13455–13470, 2014.

Dupuy, E., et al. (2009), Validation of ozone measurements from the Atmospheric Chemistry Experiment (ACE), Atmos. Chem. Phys., 9, 287–343, 2009.

Eckert, E., et al. (2014), Drift-corrected trends and periodic variations in MIPAS IMK/IAA ozone measurements, Atmos. Chem. Phys., 14, 2571–2589, 2014.

Egorova, T., et al. (2005), Influence of solar 11-year variability on chemical composition of the stratosphere and mesosphere simulated with a chemistry-climate model, Advances in Space Research 35 (2005) 451–457.

Froidevaux, L., et al. (2008), Validation of Aura Microwave Limb Sounder stratospheric ozone measurements, J. Geophys. Res., 113, D15S20, doi:10.1029/2007JD008771.

Gebhardt, C., et al. (2014), Stratospheric ozone trends and variability as seen by SCIAMACHY during the last decade, Atmos. Chem. Phys., 14, 831–846, 2014.

Jones, A., et al., (2009), Evolution of stratospheric ozone and water vapour time series studied with satellite measurements, Atmos. Chem. Phys., 9, 6055–6075, 2009.

Kerzenmacher, T., et al. (2008), Validation of $NO_2$ and NO from the Atmospheric Chemistry Experiment (ACE), Atmos. Chem. Phys., 8, 5801–5841, 2008.

Kyrola, E., et al. (2013), Combined SAGE II–GOMOS ozone profile data set for 1984–2011 and trend analysis of the vertical distribution of ozone, Atmos. Chem. Phys., 13, 10645–10658, 2013

Lambert, A., et al. (2007), Validation of the Aura Microwave Limb Sounder middle atmosphere water vapor and nitrous oxide measurements, J. Geophys. Res., 112, D24S36, doi:10.1029/2007JD008724

McCormack, J. P. D. E. Siskind, and L. L. Hood, Solar-QBO interaction and its impact on stratospheric ozone in a zonally averaged photochemical transport model of the middle atmosphere (2007) J. Geophys. Res., 112, D16109, doi:10.1029JD008369.

Nazaryan, H., M. P. McCormick, and J. M. Russell III (2005), New studies of SAGE II and HALOE ozone profile and long-term change comparisons, J. Geophys. Res., 110, D09305, doi:10.1029/2004JD005425.

Nedoluha, G. E., et al. (1998), Changes in upper stratospheric $CH_4$ and $NO_2$ as measured by HALOE and implications for changes in transport, Geophys. Res. Lett., 25, 987–990.

Newchurch, M. J., Yang, E.-S., Cunnold, D. M., Reinsel, G. C., Zawodny, J. M., and Russell III, J. M.: Evidence for slowdown in stratospheric ozone loss: first stage of ozone recovery (2003), J. Geophys. Res., 108, 4507, doi:10.1029/2003JD003471, 2003.

Olsen, S. C., C. A. McLinden, and M. J. Prather, (2001) Stratospheric $N_2O$-$NO_y$ system: Testing uncertainties in a three-dimensional framework, J. Geophys. Res., 106, D22, 28771-28784

Plummer, D. A., et al. (2010), Quantifying the contributions to stratospheric ozone changes from ozone depleting substances and greenhouse gases, Atmos. Chem. Phys., 10, 8803–8820, 2010.

Portmann, R. W., J. S. Daniel, and A. R. Ravishankara (2012), Stratospheric ozone depletion due to nitrous oxide: influences of other gases, Phil. Trans. R. Soc. B (2012) 367, 1256–1264 doi:10.1098/rstb.2011.0377

Randel, W. J., et al. (2000), Interannual changes in stratospheric constituents and global circulation derived from satellite data, in Atmospheric Science Across the Stratopause, Geophys. Monogr. Ser., vol. 123, pp. 271– 285, AGU, Washington, D. C., 2000.

Ravishankara, A. R., et al., (2009), Nitrous Oxide ($N_2O$): The dominant ozone-depleting substance emitted in the 21$^{st}$ century, Science 326, 123, DOI: 10.1126/science.1176985

Remsberg, E. E., P. P. Bhatt, and L. E. Deaver (2001), Ozone changes in the lower stratosphere from the halogen occultation experiment for 1991 through 1999, J. Geophys. Res., 106, 1639 – 1653, doi:10.1029/2000JD900596.

Remsberg, E. E. (2008), On the response of Halogen Occultation Experiment (HALOE) stratospheric ozone andtemperature to the 11-year solar cycle forcing, J. Geophys. Res., 113, D22304, doi:10.1029/2008JD010189.

Remsberg, E. and G. Lengenfelser (2010), Analysis of SAGE II ozone of the middle and upper stratosphere for its response to a decadal-scale forcing, Atmos. Chem. Phys., 10, 11779–11790, 2010.

Schmidt, H., G. P. Brasseur, and M. A. Giorgetta (2010), Solar cycle signal in a general circulation and chemistry model with internally generated quasi-biennial oscillation, J. Geophys. Res., 115, D00I14, doi:10.1029/2009JD012542.

Siskind, D. E., M. H. Stevens and C. R. Englert (2005) A model study of global variability in mesospheric cloudiness, J. Atm Solar Terr Phys., 67, 501-513.

Summers, M. E., D. E. Siskind, J. T. Bacmeister, R. R. Conway, S. E. Zasadil, and D. F. Strobel, (1997) Seasonal variation of middle atmospheric CH4 and H2O with a new chemical-dynamical model, J. Geophys. Res., 102, D3, 3503-3526.

Yang, E.-S., Cunnold, D. M., Salawitch, R. J., McCormick, M. P., Russell III, J. M., Zawodny, J. M., Oltmans, S., and Newchurch, M. J. (2006): Attribution of recovery in lower stratospheric ozone, J. Geophys. Res., 111, D17309, doi:10.1029/2005JD006371, 2006.

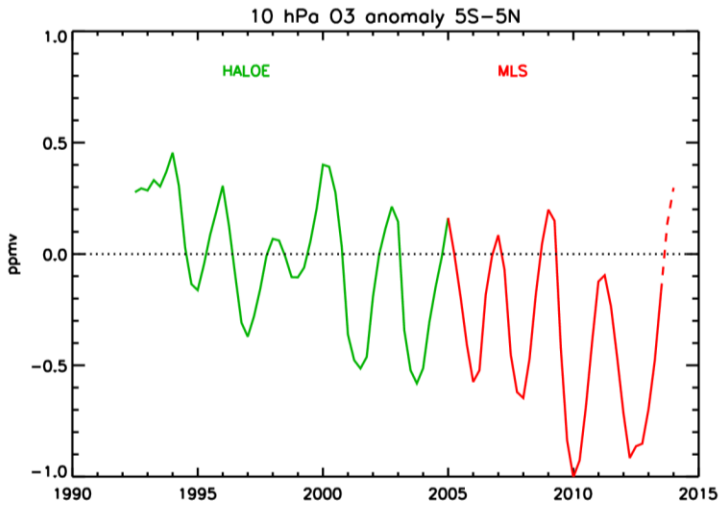


462

463 **Figure 1 - Annual median ozone anomalies at 10 hPa 5°S-5°N from HALOE (green; HALOE data is actually**
464 **shown on its native grid at 30 km, which is ~10 hPa) and MLS (red). Annual anomalies are shown four times**
465 **per year; hence each measurement is included in four datapoints. The MLS anomalies have been shifted by a**
466 **constant mixing ratio so that the HALOE and MLS annual anomalies for 2005 (covering the period July**
467 **2004-June 2005) agree. The MLS data from July 2013 onwards is indicated dashed in order to indicate that**
468 **this data will not be used in any of the linear trend calculations to be shown.**

469

470

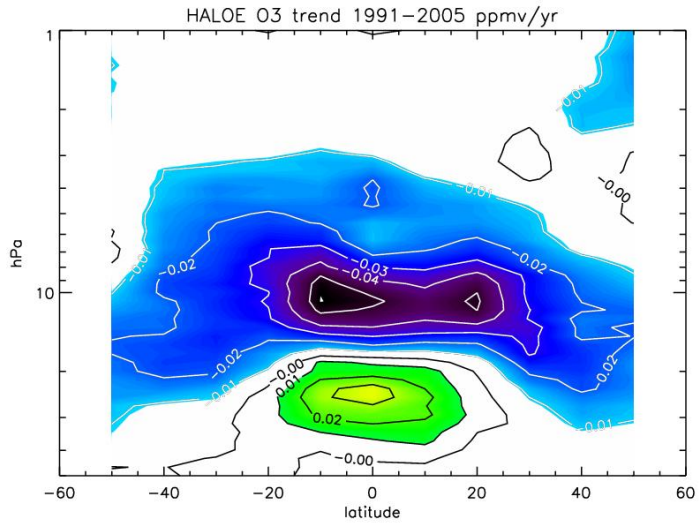


471

472 **Figure 2 - The calculated linear trend in HALOE ozone for 1991-2005. The HALOE data has been sorted**

473 **into eleven 10$^{o}$ latitude bins from 55$^{o}$S to 55$^{o}$N. Regions where the magnitude of the trend is <0.01 ppmv/year**

474 **are indicated in white.**

475

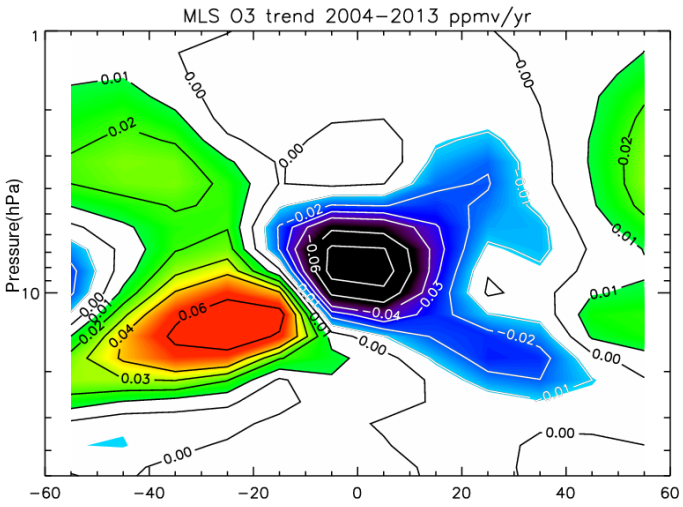


**Figure 3 – The $O_3$ linear trend calculated from MLS data from August 2004- May 2013. Contour lines are shown at +/-0.01, 0.02, 0.03, 0.04, 0.06, 0.08 ppmv/yr. The MLS data has been sorted into twelve 10° latitude bins from 60°S to 60°N. Regions where the magnitude of the trend is <0.01 ppmv/year are indicated in white.**

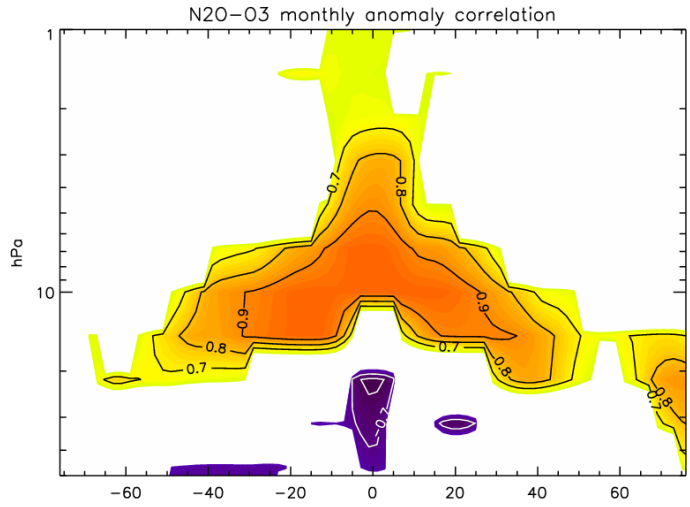


**Figure 4 – Correlation coefficients between $N_2O$ and $O_3$ calculated from monthly median anomalies from MLS data as a function of latitude and pressure. Results are shown for regions where the correlation (or anti-correlation) is >0.6.**

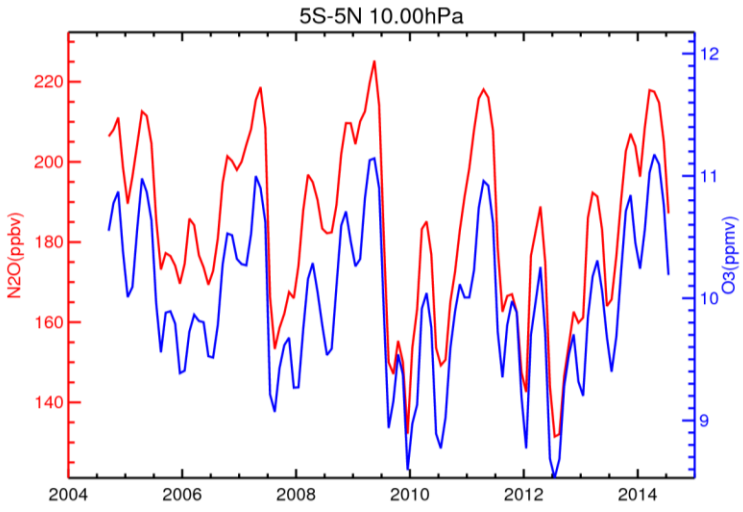


**Figure 5 – Monthly median $N_2O$ (red) and $O_3$ (blue) mixing ratios at 10 hPa from MLS measurements between 5°S and 5°N.**

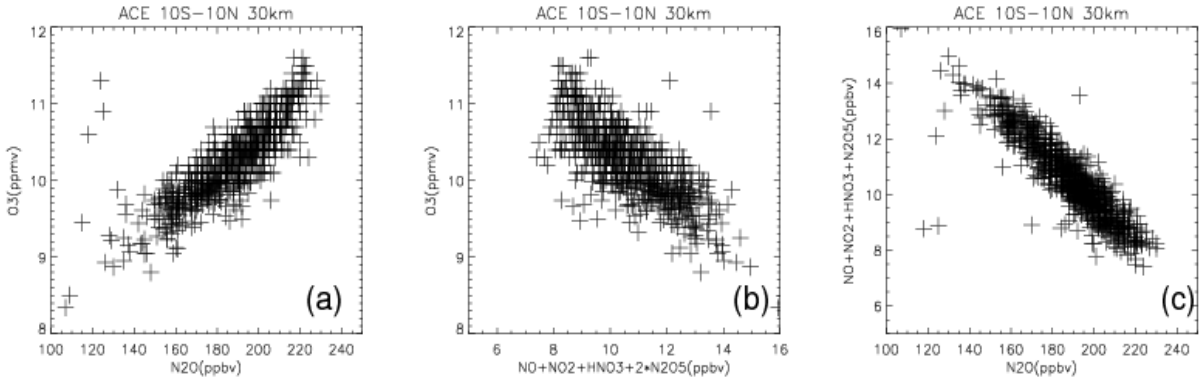


**Figure 6 – ACE measurements of $O_3$, $N_2O$, and the key members of the NOy family, $NO+NO_2+HNO_3+2*N_2O_5$. Measurements are shown for $10^oS$-$10^oN$ at 30 km. Both sunrise and sunset measurements are included.**

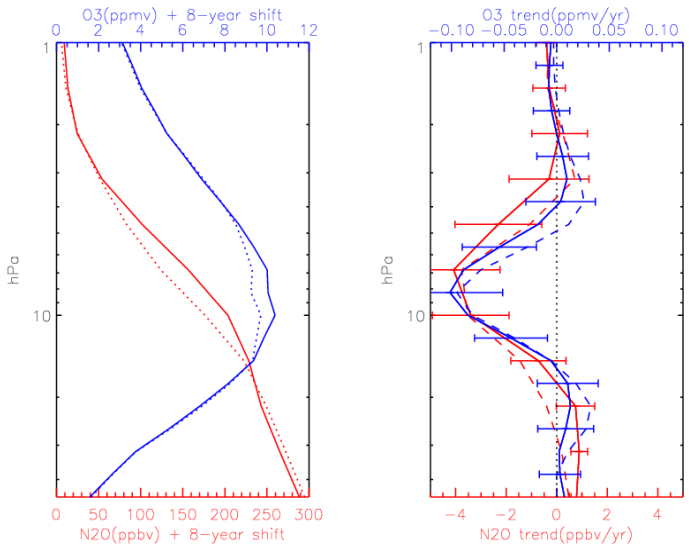


**Figure 7 - Left hand panel: Annual average MLS profiles of $O_3$ (blue; top scale) and $N_2O$ (red; bottom scale) from 5°S-5°N. Shown are the constant term derived from the fit to the August 2004- May 2013 MLS measurements (solid), and the same term with an added 8-year shift (thus approximating the difference between the 2004/5 and 2012/13 MLS annual average) based on the linear trend applied over a period comparable to the length of the MLS dataset (dotted). Right hand panel: Linear annual trend calculated with a solar cycle term included (solid) and without a solar cycle term (dashed). Error bars (2σ) are similar for fits with and without the solar cycle, and are shown only for the former.**

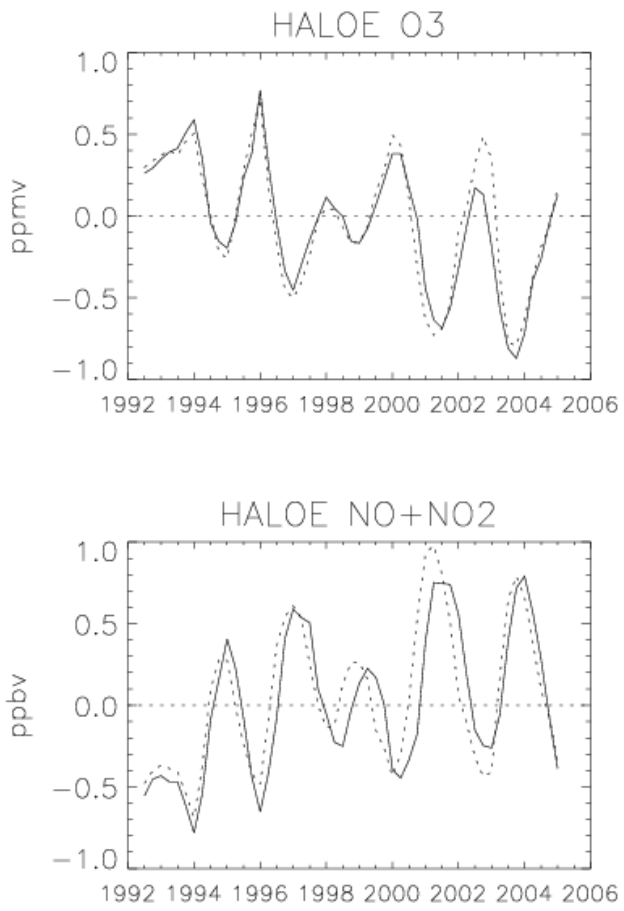


516

517 **Figure 8 - Annual median HALOE $O_3$ (top) and $NO+NO_2$ (bottom) anomalies at 10 hPa from $5^oS$-$5^oN$.**

518 **Annual anomalies are shown four times per year, hence each measurement is included in four datapoints.**

519 **Results are shown separately for sunrise (solid) and sunset (dashed). Sunset $NO+NO_2$ anomalies have been**

520 **multiplied by 0.4 so that they fit on the same scale as the sunrise anomalies.**

521

522

523

524

525

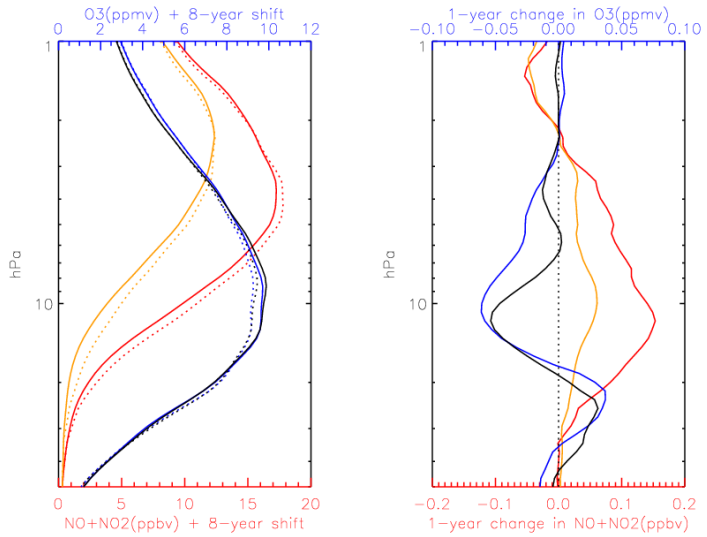


526
527

528 **Figure 9 - Left hand panel: Annual average HALOE profiles of $O_3$ at local sunset (blue; top scale), local**
529 **sunrise (black; top scale) and NO+$NO_2$ at local sunset (red; bottom scale), and local sunrise (orange; bottom**
530 **scale) from 5°S-5°N. Results are shown for the first year of HALOE measurements (solid) and with an 8-year**
531 **shift (to allow for comparison with Figure 7) using the annual average trend shown on the right-hand panel**
532 **(dashed). Right hand panel: 1-year changes based on linear trends over 5°S-5°N calculated from 1991-2005.**
533 **Line colors are the same as in the left-hand panel.**

534

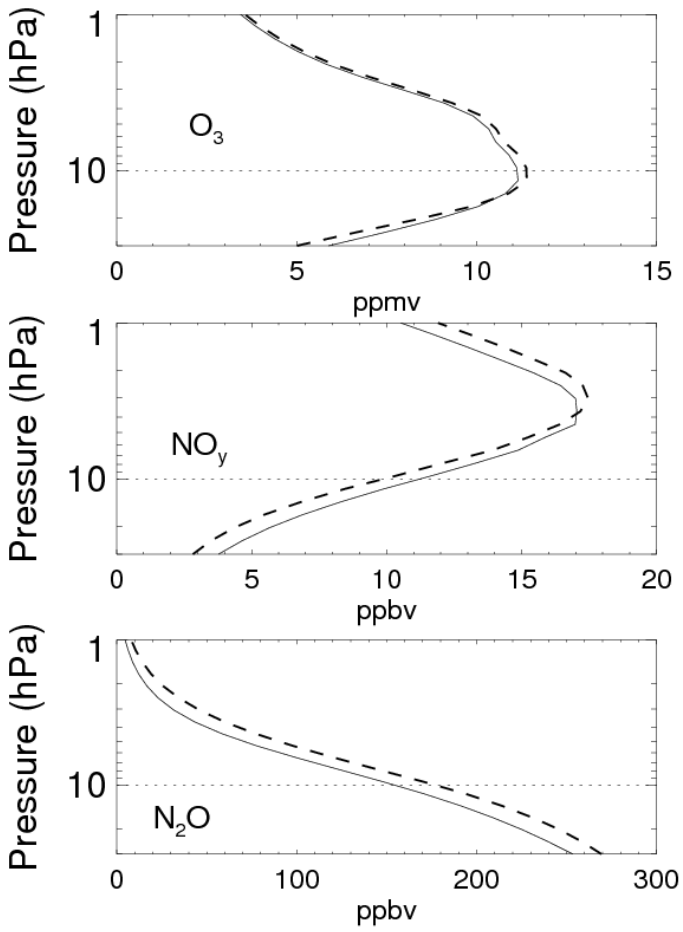


**Figure 10 - Annual average altitude profiles of $O_3$, $NO_y$, and $N_2O$ for the equator. The solid curve is a baseline run, while the dashed curve is a simulation which includes an additional 0.3 K/day heat source in the lowermost stratosphere which acts to increase the tropical upwelling.**